Journal of Alloys and Compounds 521 (2012) 1–3

Contents lists available at SciVerse ScienceDirect

Journal of Alloys and Compounds

journal homepage: www.elsevier.com/locate/jallcom

Letter

Crystal structure of the ternary Mg–Zn–Ce phase in rapidly solidified Mg–6Zn–1Y–1Ce alloy

W.P. Yang[a,b,*], X.F. Guo[a], Z.X. Lu[b]

[a] School of Materials Science and Engineering, Henan Polytechnic University, Jiaozuo, Henan 454000, China
[b] School of Materials Science and Engineering, Xi'an University of Technology, Xi'an, Shaanxi 710048, China

ARTICLE INFO

Article history:
Received 10 April 2011
Received in revised form
26 December 2011
Accepted 28 December 2011
Available online 21 January 2012

Keywords:
Crystal structure
TEM
Phase transitions

ABSTRACT

Transmission electron microscopy and energy dispersive X-ray spectroscopy were employed to characterize the composition and crystal structure of ternary Mg–Zn–Ce phase (denoted as T1) in rapidly solidified Mg–6Zn–1Y–1Ce alloy. T1 phase was confirmed having a body-centered orthorhombic structure, which was transformed from the body-centered tetragonal structure $Mg_{12}Ce$ phase due to the partial substitution of Mg atoms by Zn. An orientation relationship between T1 phase and matrix was that $\langle 1\,0\,0\rangle_{T1} \parallel \langle 1\,0\,-1\,0\rangle_{\alpha}$, $\langle 0\,1\,0\rangle_{T1} \parallel \langle -1\,2\,-1\,0\rangle_{\alpha}$, $\langle 0\,0\,1\rangle_{T1} \parallel \langle 0\,0\,0\,1\rangle_{\alpha}$. Under non-equilibrium condition, the contents of Zn and Ce in T1 phase were in the ranges of 28.9–45.3 at.% and 7.6–10.4 at.%, respectively.

1. Introduction

Mg alloys have great potential for high performance aerospace and automotive applications owing to their low density, high specific strength and stiffness [1]. However, Mg alloys produced by traditional ingot metallurgy exhibit low strength, ductility and creep resistance due to coarse dendrites and brittle intermetallic networks at grain boundaries [2,3]. An alternative way to refine the microstructure is using rapidly solidified powder metallurgy (RS/PM) technology. RS/PM Mg alloys with the addition of rare earth (RE) show significant improvement on mechanical properties at room temperature and elevated temperatures due to the fine microstructure and formation of high melting point intermetallic particles [4–9]. For Mg–Zn–RE system, Mg–Zn–Y–Ce alloys seem particularly promising because their microstructures are stable around 300 °C [5], and they exhibit high strengths and sufficient elongations depending on preparation process. RS/PM Mg–6Zn–1Y–0.6Ce–0.6Zr alloy prepared by extrusion has high tensile strengths of 490–520 MPa and elongations of 6–10% [7]. The alloy processed by reciprocating extrusion exhibits a high elongation of 27% and a high strength of 340 MPa. Interestingly, this alloy also shows two distinct yield points [4]. Besides the refine-grained microstructure, mechanical properties of materials mostly depend on the structural characteristics of their strengthening particles. Previous reports [5–7] comparatively studied the microstructures of rapidly solidified (RS) Mg–Zn–Y and Mg–Zn–Y–Ce ribbons, and found that Ce plays an important role on the microstructural refinement and resultant improvement on mechanical properties of the consolidated materials due to the limited solubility of Ce in Mg. In this paper, we report on the structural characteristics of the Ce-contained phase in RS Mg–6Zn–1Y–1Ce ribbon using transmission electron microscopy (TEM).

2. Experimental procedure

An Mg–6Zn–1Y–1Ce ingot was prepared by melting Mg (99.9%), Zn (99.9%), master alloys of Mg–47%Y and Mg–90%Ce under Ar atmosphere. The as-cast alloy was remelted in a plain carbon steel crucible wrapped in a high frequency induction heating coil at 720 °C in a low Ar pressure atmosphere of 4.4×10^2 Pa, and then the melt was injected through a nozzle with a gap width of ~1 mm onto the surface of a spinning copper wheel with a circumferential speed of ~22 m/s. The thicknesses of the produced ribbons were about 100 μm and cooling rate was estimated to be about 1.65×10^6 °C/s according to the cooling rate function [10]. TEM specimen was twin-jet electron-polished to perforation, finally ion-milled to remove the fine oxide film at an ion accelerating voltage of 4 keV. TEM observation was carried out using a JEM-3010 equipped with an Oxford Instruments energy-dispersive X-ray (EDX) spectrometer operating at 300 kV.

3. Results and discussions

Fig. 1a shows a bright-field TEM image taken from RS ribbon. An EDX spectrum (Fig. 1b) recorded from the particle indicated by an arrow in Fig. 1a revealed the prominent Mg K_α and Zn K_α peaks, significant intensity of Zn L_α peak, and low intensities of Ce L_α, L_β

* Corresponding author at: Henan Polytechnic University, School of Materials Science and Engineering, Century Avenue, No. 2001, Jiaozuo, Henan 454000, China. Tel.: +86 391 3986906; fax: +86 391 3986906.
E-mail address: wenpengy@gmail.com (W.P. Yang).

0925-8388/$ – see front matter © 2012 Elsevier B.V. All rights reserved.
doi:10.1016/j.jallcom.2011.12.144

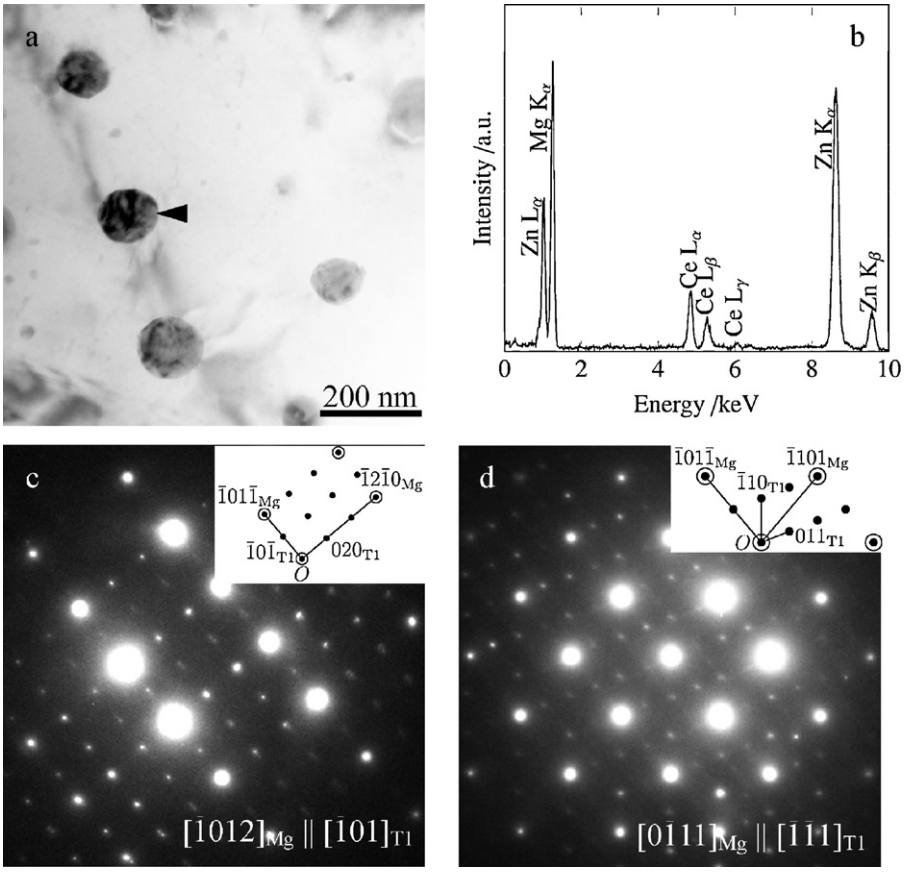

Fig. 1. (a) A BF TEM image taken from WS region; (b) an EDX spectrum recorded from the T1 phase particle indicated by an arrow in (a); (c) a set of composite SAED patterns of the particle and surrounding matrix taken from [−1 0 1 2] zone axis of Mg; (d) a set of composite SAED patterns taken from [0 −1 1 1] zone axis after titling 39.7° along {1 0 −1 1} vector from [−1 0 1 2] zone axis.

and Zn K_β peaks. The composition of the particle was determined to be Mg–43.1 at.%Zn–8.6 at.%Ce, which approached to those of $(MgZn)_{12}Ce$ [11] and T phase [12,13]. $(MgZn)_{12}Ce$ phase is a continuous substitutional solid solution of $Mg_{12}Ce$ phase by exchanging Mg atoms by Zn, and the solid solubility limit of Zn is 48.49 at.% at 350 °C [11]. Earlier, Drits et al. [14] suggested that T phase is a solid solution of $Mg_{17}Ce_2$ phase with the $Th_{17}Ni_2$ type structure (a = 10.10 Å, c = 9.97 Å, space group $P6_3/mmc$). Thereafter, Wei et al. [12] indicated that T phase has a c-centered orthorhombic structure (a = 9.6 Å, b = 11.2 Å, c = 9.4 Å in the Mg–8Zn–1.5 MM (misch metal) alloy, and a = 10.1 Å, b = 11.6 Å, c = 9.9 Å in the Mg–5Zn–10 MM alloy). To avoid confusion, in this paper the ternary Mg–Zn–Ce phase was denoted as T1 phase. Fig. 1c shows the composite SAED patterns recorded from the particle and surrounding matrix indicated by the arrow in Fig. 1a. The strong diffraction spots were indexed consistently according to be α-Mg (a = 3.09 Å, c = 5.00 Å) with the electron beam (EB) parallel to [−1 0 1 2] zone axis. The weak spots have perfect orientation relationships with matrix. However, the pattern of the T1 phase could not be indexed to neither $Mg_{12}Ce$ nor T phase. The strong SAED spots shown in Fig. 1d was recorded from [0 −1 1 1] zone axis that was arrived at by tilting about 39.7° along the {1 0 −1 1} matrix vector from [−1 0 1 2] zone axis. The SAED pattern of the particle also matched well with that of matrix.

According to the composite diffraction patterns of matrix and T1 phase in Fig. 1c and d, a reciprocal space lattice of the T1 phase could be built based on the frame of the reciprocal lattice of Mg matrix. Fig. 2 shows a schematic diagram of composite reciprocal lattices of matrix and T1 phase with their vectors $\boldsymbol{c}^*$ up perpendicular to paper. It is clear from Fig. 2 that the reflections of T1 phase satisfying the condition of $h + k + l = 2n + 1$ were absent and that the reciprocal lattice showed a face-centered orthorhombic structure. Reversely, the corresponding crystal structure in real space was a body-centered orthorhombic structure. Hence, the diffraction patterns of T1 phase in Fig. 1c and d could be indexed according to the analysis result of Fig. 2, as shown in the inserts in Fig. 1c and d. In turn, the lattice parameters of T1 phase could be calculated ($a_{T1} \approx \sqrt{3}\, a_{Mg}$ = 5.35 Å, $b_{T1} \approx 3\, a_{Mg}$ = 9.43 Å, $c_{T1} \approx 2\, c_{Mg}$ = 10.02 Å, space group $Immm$). With the lattice parameters of α-Mg and T1 phase calculated in this paper, we calculated the stereographic projects for the present orientation relationship, as shown in Fig. 3. Their orientation

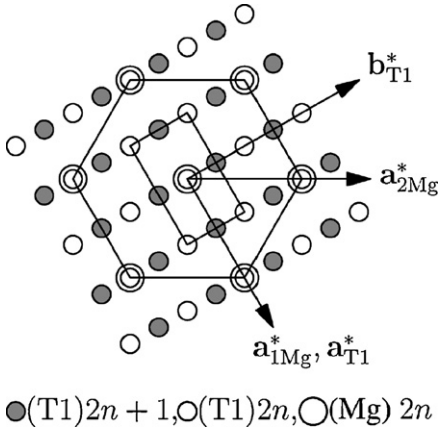

Fig. 2. A schematic diagram of composite reciprocal lattices of α-Mg and T1 phase.

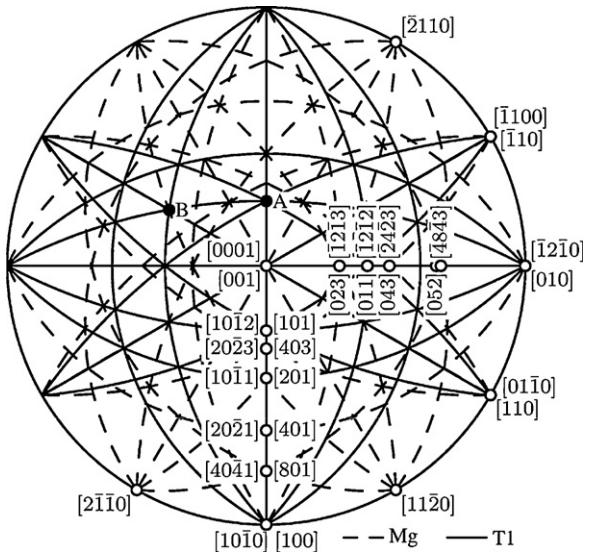

Fig. 3. The stereographic projects of α-Mg and T1 phase for the present orientation relationship.

relationship was in the form that $\langle 1\,0\,0\rangle_{T1} \parallel \langle 1\,0\,-1\,0\rangle_{\alpha}$, $\langle 0\,1\,0\rangle_{T1} \parallel \langle -1\,2\,-1\,0\rangle_{\alpha}$, $\langle 0\,0\,1\rangle_{T1} \parallel \langle 0\,0\,0\,1\rangle_{\alpha}$. The zone axes of matrix and T1 phase in Fig. 1c and d were pointed out in Fig. 3 by labels A and B, respectively.

In RS Mg–6Zn–1Y–1Ce alloy, almost all Ce atoms were captured by T1 phase. The $Mg_{17}Ce_2$ phase, which was detected by X-ray diffraction in previous report [6], was not found in present study. The present work identifies T1 phase was a body-centered orthorhombic structure. Its calculated crystallographic data approximated to that of body-centered tetragonal structure $Mg_{12}Ce$ phase (a = 10.33 Å, c = 5.96 Å, space group $I4/mmm$). Since the radius of Zn atom (1.53 Å) is smaller than that of Mg (1.72 Å) atom, when Mg atoms are substituted by Zn, the lattice parameters should have a little decrease and the body-centered tetragonal structure could transform into body-centered orthorhombic structure. Therefore, it is confident to conclude that the T1 phase was the solid solution of $Mg_{12}Ce$ phase. Further, it could be concluded that the more Zn atoms the T1 phase contained, the smaller lattice parameters the T1 phase had. In addition, We examined a number of T1 phase particles and found that there was a composition fluctuation in T1 phase, and the contents of Zn and Ce were in the ranges of 28.9–45.3 at.% and 7.6–10.4 at.%, respectively. The content deviations of Zn and Ce among T1 phase particles could be attributed to the nonequilibrium solidification process.

4. Conclusions

In RS Mg–6Zn–1Y–1Ce alloy, almost all Ce atoms were captured by the ternary Mg–Zn–Ce (T1) phase. The contents of Zn and Ce in T1 phase were in the ranges of 28.9–45.3 at.% and 7.6–10.4 at.%, respectively. T1 phase had a body-centered orthorhombic structure ($a_{T1} \approx \sqrt{3}\ a_{Mg}$ = 5.35 Å, $b_{T1} \approx 3\ a_{Mg}$ = 9.43 Å, $c_{T1} \approx 2\ c_{Mg}$ = 10.02 Å, space group $Immm$), and an orientation relationship between T phase and matrix was that $\langle 1\,0\,0\rangle_{T} \parallel \langle 1\,0\,-1\,0\rangle_{\alpha}$, $\langle 0\,1\,0\rangle_{T} \parallel \langle -1\,2\,-1\,0\rangle_{\alpha}$, $\langle 0\,0\,1\rangle_{T} \parallel \langle 0\,0\,0\,1\rangle_{\alpha}$.

Acknowledgements

The authors gratefully acknowledge the support of (a) National Natural Science Foundation of China (50271054), (b) Ph.D. Programs Foundation of Ministry of Education of China (20070700003), (c) Science and Technologies Foundation of He'nan of China (102102210031) and (d) Natural Science Foundation of He'nan Educational Committee of China (2010A430008).

References

[1] P. Bolt, N. Lamboo, P. Rozier, J. Mater. Proc. Technol. 115 (2001) 2–8.
[2] W. Xiao, S. Jia, L. Wang, Y. Wu, L. Wang, J. Alloys Compd. 480 (2009) 33–36.
[3] W. Xiao, J. Wang, J. Yang, S. Jia, L. Wang, Mater. Sci. Eng. A 485 (2008) 55–60.
[4] X. Guo, D. Shechtman, J. Mater. Proc. Technol. 187/188 (2007) 640–644.
[5] X. Guo, S. Remennik, C. Xu, D. Shechtman, Mater. Sci. Eng. A 473 (2008) 266–273.
[6] X. Guo, D. Shechtman, Glass Phys. Chem. 31 (2005) 44–52.
[7] X. Guo, J. Kinstler, L. Glazman, D. Shechtman, Mater. Sci. Forum 488/489 (2005) 495–498.
[8] E. Mora, G. Garcés, E. Oñorbe, P. Pérez, P. Adeva, Scr. Mater. 60 (2009) 776–779.
[9] V. Šustek, S. Spigarelli, J. Cadek, Scr. Mater. 35 (1996) 449–454.
[10] X.J. Wang, X.D. Chen, T.D. Xia, W.Y. Yu, X.L. Wang, Intermetallics 12 (2004) 1233–1237.
[11] D. Kevorkov, M. Pekguleryuz, J. Alloys Compd. 478 (2009) 427–436.
[12] L.Y.Wei, G.L. Dunlop, H. Westengen, Metal. Mater. Trans. 26 (1995) 1947–1955.
[13] L.Y. Wei, G.L. Dunlop, J. Mater. Sci. Lett. 15 (1996) 4–7.
[14] M.E. Drits, E.I. Drozdova, I.G. Korol'kova, V.V. Kinzhibalo, A.T. Tyvanchuk, Russ. Metall. 2 (1989) 195–197.